NeuroImage: Clinical 16 (2017) 468–476

Contents lists available at ScienceDirect

NeuroImage: Clinical

journal homepage: www.elsevier.com/locate/ynicl

General and selective brain connectivity alterations in essential tremor: A resting state fMRI study

Karsten Mueller[a,1], Robert Jech[b,*,1], Martina Hoskovcová[b], Olga Ulmanová[b], Dušan Urgošík[c], Josef Vymazal[c], Evžen Růžička[b]

[a] Max Planck Institute for Human Cognitive and Brain Sciences, Leipzig, Germany
[b] Department of Neurology, Charles University, First Faculty of Medicine and General University Hospital in Prague, Czech Republic
[c] Na Homolce Hospital, Prague, Czech Republic

ARTICLE INFO

Keywords:
Essential tremor
Magnetic resonance imaging
fMRI
Brain connectivity
Eigenvector centrality
Fahn-Tolosa-Marin Tremor Rating Scale

ABSTRACT

Although essential tremor is the most common movement disorder, there is little knowledge about the pathophysiological mechanisms of this disease. Therefore, we explored brain connectivity based on slow spontaneous fluctuations of blood oxygenation level dependent (BOLD) signal in patients with essential tremor (ET). A cohort of 19 ET patients and 23 healthy individuals were scanned in resting condition using functional magnetic resonance imaging (fMRI). *General connectivity* was assessed by eigenvector centrality (EC) mapping. *Selective connectivity* was analyzed by correlations of the BOLD signal between the preselected seed regions and all the other brain areas. These measures were then correlated with the tremor severity evaluated by the Fahn-Tolosa-Marin Tremor Rating Scale (FTMTS). Compared to healthy subjects, ET patients were found to have lower EC in the cerebellar hemispheres and higher EC in the anterior cingulate and in the primary motor cortices bilaterally. In patients, the FTMTS score correlated positively with the EC in the putamen. In addition, the FTMTS score correlated positively with selective connectivity between the thalamus and other structures (putamen, pre-supplementary motor area (pre-SMA), parietal cortex), and between the pre-SMA and the putamen. We observed a selective coupling between a number of areas in the sensorimotor network including the basal ganglia and the ventral intermediate nucleus of thalamus, which is widely used as neurosurgical target for tremor treatment. Finally, ET was marked by suppression of general connectivity in the cerebellum, which is in agreement with the concept of ET as a disorder with cerebellar damage.

1. Introduction

Although essential tremor (ET) is the most common movement disorder, its causes and pathophysiological mechanisms are still unknown. For the development of new approaches of ET therapy, a better understanding of the pathophysiological background would be crucial. In particular, the mechanisms behind altered brain oscillations need to be further studied. Investigating ET relating to resting brain connectivity changes might be essential for understanding the whole picture of ET even in the absence of tremor when a patient has their arms in a relaxed position.

In our study, we investigated whole brain connectivity alterations with ET using resting-state fMRI from two perspectives. First, we used eigenvector centrality (EC) as a measure of *general connectivity* in order to investigate a potential change of interconnectedness between brain regions of ET patients. Second, we analyzed voxel-wise correlations from predefined seeds in motor network with a complementary approach as a measure of *selective connectivity*. While the *general connectivity* is based on data driven analysis of resting network in ET, the *selective connectivity* analyzes a limited number of connections based on a priori hypotheses.

The method of EC was established for analysis of resting-state fMRI data to detect major hubs of brain networks using correlations between fMRI time courses (Lohmann et al., 2010). Higher EC values are attributed to brain regions which show a high connectivity with other brain regions having higher EC values themselves. In contrast to other methods for investigating brain connectivity using selected fMRI time courses of specific brain regions (Friston et al., 2003; Lohmann et al., 2012), the concept of EC works without a priori assumptions by using all measured fMRI time courses within the data set. Thus, the procedure

* Corresponding author at: Center for interventional therapy of movement disorders, Department of Neurology, Charles University, First Faculty of Medicine and General University Hospital in Prague, Kateřinská 30, 120 00 Praha, Czech Republic.
E-mail address: jech@cesnet.cz (R. Jech).
[1] Equal contribution.

http://dx.doi.org/10.1016/j.nicl.2017.06.004
Received 9 February 2017; Received in revised form 22 May 2017; Accepted 1 June 2017
Available online 02 June 2017

can be used to detect disease-related brain connectivity changes based on resting-state fMRI. Meanwhile, EC is successfully used in various fields of neurodegenerative disease such as Alzheimer's disease and mild cognitive impairment (Binnewijzend et al., 2014; Qiu et al., 2016) but also within movement disorders such as Parkinson's disease (Holiga et al., 2015; Lou et al., 2015). However, to our knowledge, no work has yet used EC to investigate ET functional correlates with respect to clinical involvement.

The ET can be treated with deep brain stimulation or lesioning of the ventral intermediate nucleus (VIM) of the thalamus if tremor is unbearable. This structure is well known to be related to tremor oscillatory network (Hassler and Riechert, 1954). Recently, that brain structure was confirmed to play a central role in ET demonstrating connectivity alterations between VIM and other brain regions within the thalamo-cortical-cerebellar network (Fang et al., 2016). We included the VIM to seed-based correlation analysis to map *selective connectivity*, considering the potential relationship between tremor severity and brain connectivity between VIM and other brain regions within the motor system. Further hypotheses assumed involvement of several cortical regions in the motor network potentially participating in ET pathophysiology regardless of *general connectivity* dysfunction. Therefore, *selective connectivity* was investigated using additional seeds including the supplementary motor area (pre-SMA, post-SMA), lateral premotor cortex (LPM), primary motor cortex (M1) and primary somatosensory cortex (S1) with locations derived from previously published meta-analysis of 126 papers (Mayka et al., 2006) as some of these regions were previously attributed to ET dysfunction (Neely et al., 2015).

2. Methods

2.1. Participants

A cohort of 19 patients with ET (55.5 ± (SD) 19.2 years, disease duration: 6–54 years) and 23 healthy individuals (50.9 ± 18.0 years) were included in the study. All patients fulfilled the clinical criteria for the diagnosis of ET (Deuschl et al., 1998). Thirteen patients (68%) reported a positive family history of tremor. Nine patients were on regular monotherapy or combined treatment to suppress tremor (5 on beta-sympatholytics, 5 on primidone, 5 on benzodiazepines and 2 on gabapentin) which they were taking on the day of examination, while 10 patients weren't taking any drugs for tremor. All subjects were without history or clinical signs of any other neurological or psychiatric disorders. The study protocol was approved by the Ethics Committee of the General University Hospital in Prague, Czech Republic. All participants were carefully informed about the study and signed a written consent in accordance with the Declaration of Helsinki.

2.2. Clinical assessment

All patients underwent clinical assessment investigating the tremor severity using the Fahn-Tolosa-Marin Tremor Rating Score (FTMTS) (Fahn et al., 1993) with an average total score of 28.8 ± 15.3. Here we assessed the tremor in the left and right arms and legs, head, voice, and trunk. While resting tremor was assessed with relaxed arms on knees of patients with siting position, postural tremor was evaluated with arms raised horizontally forward with hands pronated. To assess kinetic tremor, the finger-to-nose task was performed with each upper limb. Patients mainly suffered with nearly symmetrical postural tremor (1.6 ± 0.7) and kinetic tremor (1.7 ± 0.7) of arms, while the resting component was only minimally expressed (0.2 ± 0.4). An additional clinical description of all patients is listed in Table 1.

2.3. Resting state fMRI protocol

All subjects were scanned with resting-state fMRI protocol in supine position with the eyes open fixating the cross in the middle of the visual field. As their upper limbs were freely positioned along trunk in relaxed state, the resting tremor was absent or negligible (see above). Wakefulness of each subject was continuously monitored with the MRI compatible camera 12 M (MRC Systems, Heidelberg, Germany) aiming at the left eyeball throughout the whole scanning session. Imaging data were obtained using a 1.5 T MAGNETOM Avanto scanner (Siemens Healthcare, Erlangen, Germany) with a T2*-weighted gradient-echo echo planar imaging (EPI) sequence (repetition time, TR = 3 s; echo time, TE = 51 ms, flip angle 90°) with an acquisition of 200 volumes in a period of 10 min. Each volume consisted of 31 axial slices (thickness = 3 mm, gap = 1 mm) with a nominal in-plane resolution of $3 \times 3\,mm^2$ covering the whole brain. For registration purposes, *T1*-weighted images were obtained using a magnetization-prepared rapid gradient echo (MP-RAGE) sequence (TR = 2140 ms; inversion time, TI = 1100 ms; TE = 3.93 ms; flip angle 15°). A set of 176 sagittal slices were acquired with a nominal resolution of $1 \times 1 \times 1\,mm^3$.

2.4. Data pre-processing

Image pre-processing was performed using SPM8 (Wellcome Trust Centre for Neuroimaging, UCL, London, UK) and Matlab® (The MathWorks Inc., Natick, MA). Standard processing included realignment, slice-time correction, normalization to the Montreal Neurological Institute (MNI) space based on the unified segmentation approach (Ashburner and Friston, 2005). After normalization, the resulting voxel size of the functional images was interpolated to an isotropic voxel size of $3 \times 3 \times 3\,mm^3$. Spatial filtering was performed using a Gaussian kernel with 8-mm full width at half maximum. Finally, a baseline correction was achieved using a high pass filter with a cutoff frequency of 1/80 Hz. Note that it is shown that temporal filtering induces a correlation in resting-state fMRI (Davey et al., 2013) and therefore the cutoff frequency should be chosen that low frequency oscillations are not affected in the signal (Obrig et al., 2000).

2.5. General connectivity analysis

After pre-processing, the *general connectivity* of functional images was assessed by Eigenvector centrality (EC) which was computed using the Lipsia software package (Lohmann et al., 2001). EC is a suitable method for investigating hubs of networks within the whole brain (Lohmann et al., 2001; Power et al., 2013) based on a node centrality approach accentuating correlations with nodes that are central within the network (Lohmann et al., 2010). EC attributes a value to each voxel in the brain so that a voxel receives a large value if it is strongly correlated with many other nodes that are themselves central within the network. Using the EC measure, an EC map can be produced in which each voxel has a value that indicates its centrality. For obtaining an EC, a similarity matrix $\boldsymbol{A} = [a_{ij}]$ was computed including Pearson's correlation coefficient between all resting-state fMRI time courses for the whole brain. In order to use a similarity matrix with only positive numbers, the absolute value was taken from all correlation coefficients before computing the EC. Thus, we achieved $a_{ij} > 0$ for all elements of the similarity matrix $\boldsymbol{A}$. According to the theorem of Peron and Frobenius (Frobenius, 1912), this similarity matrix has a unique real largest eigenvalue λ, and the corresponding eigenvector has strictly positive components. Then, the EC map was generated using the *i*-th component of this eigenvector to obtain the EC value for voxel *i* as follows:

$$x_i = \mu \sum_j a_{ij} x_j \text{ with } \mu = 1/\lambda.$$

After computing EC maps for all patients and all healthy controls, a group analysis was performed using a two-sample *t*-test to check for EC differences between both groups. The resulting statistical parametric maps were processed using a voxel-wise threshold of $P < 0.005$. We

Table 1
Demographical information of the ET patients.

	Age	Sex	Age onset	Duration	FTMTS A	FTMTS B	FTMTS C	FTMTS total	T right arm	T left arm	T both arms	T right leg	T left leg	T legs	T head	T voice	T axial	Family history	Alcohol
P1	48	F	42	6	6	7	3	**16**	2	2	**4**	0	0	**0**	0	0	0	1	0
P2	55	M	29	26	7	9	2	**18**	2	2	**4**	1	1	**2**	0	1	1	1	0
P3	68	M	14	54	8	9	2	**19**	4	2	**6**	0	0	**0**	0	2	2	1	0
P4	67	M	53	14	7	11	3	**21**	3	4	**7**	0	0	**0**	0	0	0	1	1
P5	73	F	20	53	17	28	20	**65**	7	7	**14**	1	1	**2**	0	1	1	1	1
P6	47	M	16	30	10	10	4	**24**	4	4	**8**	0	0	**0**	0	2	2	0	1
P7	28	M	22	6	8	9	4	**21**	4	3	**7**	0	0	**0**	0	0	1	1	1
P8	77	M	66	11	10	17	8	**35**	3	4	**7**	1	1	**2**	0	1	1	0	0
P9	75	M	56	19	10	15	12	**37**	3	3	**6**	0	0	**0**	0	4	4	0	1
P10	65	M	42	23	12	10	2	**24**	2	2	**4**	0	0	**0**	6	2	8	1	1
P11	19	M	9	10	8	10	1	**19**	4	4	**8**	0	0	**0**	0	0	0	0	1
P12	27	F	10	17	9	11	1	**21**	3	6	**9**	0	0	**0**	0	0	0	1	1
P13	40	M	20	20	8	13	6	**27**	3	3	**6**	0	0	**0**	0	2	2	1	0
P14	81	F	40	41	25	28	14	**67**	6	6	**12**	1	1	**2**	6	2	11	0	1
P15	65	M	20	45	8	14	3	**25**	4	3	**7**	0	0	**0**	0	0	0	0	1
P16	26	M	18	8	11	3	1	**15**	2	2	**4**	1	1	**2**	0	0	4	0	0
P17	62	M	53	9	6	7	3	**16**	3	2	**5**	0	0	**0**	0	0	0	0	0
P18	68	M	55	13	19	14	12	**45**	6	5	**11**	0	0	**0**	6	2	8	1	1
P19	63	M	54	9	15	14	3	**32**	3	4	**7**	1	1	**2**	6	0	6	1	0

Abbreviations: FTMTS Fahn-Tolosa-Marin Rating Scale; FTMS A – tremor rating (item 1–9) FTMS B – action tremor of upper extremities (writing, drawing, water pouring – item 10–14) FTMS C functional disabilities due to tremor (item 15–21) total – sum of the FTMS A, B and C; T right/left arm – sum of item 5 or 6 for resting, postural and action + intentional tremor of the right or left upper extremity; T both arms – sum of the T right arm and T left arm scores; T right/left leg – sum of item 8 or 9 for resting, postural and action + intentional tremor of the right or left upper extremity; T both legs – sum of the T right arm and T left arm scores; T head – sum of the item 4 for resting and postural tremor; T voice – item 3 for action + intentional tremor; T axial – sum of items for face, tongue, head, voice, trunk and orthostatic tremor; family history – positive (1), negative (0); alcohol – suppressive effect on tremor (1), no effect on tremor (0).

also checked for multiple comparisons using family-wise error (FWE) correction with $P < 0.05$ (Nichols and Hayasaka, 2003). In addition to this FWE approach implemented in SPM8 that is relying on the assumptions of the Gaussian Random Field theory, we also used the Lipsia software (Lohmann et al., 2001) to obtain significant clusters. Here, statistical maps underwent a multiple-comparison procedure for significance thresholding based on Monte Carlo simulations with 10,000 iterations. This method uses two features (cluster size and cluster maximum) to quantify a cluster as significant (Forman et al., 1995; Poline et al., 1997). Significant clusters were obtained using a voxel-threshold of $P < 0.005$ and a corrected cluster threshold of $P < 0.05$.

We further investigated the relationship between EC and tremor severity using the FTMTS within the group of ET patients. A correlation analysis was performed between EC und FTMTS using the general linear model including age and gender as additional covariates. A significant correlation was detected using a voxel threshold of $P < 0.005$ and an FWE-corrected cluster threshold of $P < 0.05$.

In order to discuss the contribution of positive and negative correlations in context of *general connectivity* (Goelman and Dan, 2017), EC was computed using a different approach of treating correlations in the similarity matrix. In our main approach, we used the absolute value of all correlations that regards negative correlations as important as positive ones (see above). To estimate the share of negative correlations on our main result, we performed a subsequent analysis, in which we ignored all negative correlations setting all negative correlations to zero. This approach considered only the positive correlations when computing the EC. To compare both approaches, all computations including voxel-wise two-sample *t*-tests between the EC of patients and control subjects were performed with the Lipsia software package (Lohmann et al., 2001) using a voxel threshold of $P < 0.005$ and a cluster threshold of 50 voxels. We also used both approaches when computing the voxel-wise correlation between EC und FTMTS.

2.6. Selective connectivity analysis

The *selective connectivity* was mapped using seed-based correlation analysis aimed at investigating functional connectivity between preselected seed-region and other regions within the whole brain. In our seed-based analysis, coordinates for seed-voxels were chosen in the VIM nucleus of the thalamus (Klein et al., 2012), and in the premotor and sensorimotor cortices reported in meta-analysis (Mayka et al., 2006). For each ET patient, a correlation between those seeds and the rest of the brain was computed with Pearson's correlation coefficient using the LIPSIA software package (Lohmann et al., 2001). To ensure a Gaussian distribution for subsequent statistical analysis, the resulting correlation maps were transformed using the Fisher's r-to-z transform. All resulting individual correlation maps were subsequently processed in a second-level analysis using the general linear model including FTMTS, age and gender as covariates. Statistical analysis was performed using SPM8 to find a significant correlation between FTMTS and *selective connectivity* for all seed regions. A significant correlation between *selective connectivity* and the FTMTS was detected using a voxel-threshold of $P < 0.005$ and an FWE-corrected cluster threshold of $P < 0.05$. In addition, we used the Lipsia software for statistical analysis correcting for multiple comparisons with Monte Carlo simulations using a cluster threshold of $P < 0.05$.

2.7. Motion effects

Head motion inside the MR scanner might bias the connectivity analysis and, finally, the EC values due to motion-induced signal fluctuations. This could particularly be a problem if the degree of motion-related artifacts would vary between ET patients and healthy controls. Therefore, we checked for differences in head motion by computing the framewise displacement (FD) as introduced in (Power et al., 2012). As an input, we used the translational and rotational motion parameters obtained by SPM's motion correction. For the whole series of 200 functional images, motion between the volumes was characterized using 199 FD values. Finally, for both patients and controls, all FD time courses were characterized by the mean FD, the maximum FD, the maximum FD after eliminating the largest 5% of the FD values, and the number of FD values exceeding 1 mm. The difference in head motion between patients and controls was also assessed using statistical analysis. Three two-sample *t*-tests were performed to detect differences between (1) the mean FD, (2) the maximum FD, and (3) the maximum FD after eliminating the largest 5% of the FD values between patients and controls.

To investigate the effect of motion to EC, we performed a scrubbing technique using an FD threshold of 0.5 mm (Power et al., 2012). Scrubbing was performed by deleting the affected volume but also the preceding and the subsequent volume. Thus, three volumes were deleted for each single motion. For comparing EC differences using the scrubbing and the non-scrubbing approach, all computations including voxel-wise two-sample *t*-tests between the EC of patients and control subjects were performed with the Lipsia software package (Lohmann et al., 2001) using a voxel threshold of $P < 0.005$ and a cluster threshold of 20 voxels. We also computed the voxel-wise correlation between EC und FTMTS with and without the scrubbing technique.

3. Results

The group analysis including ET patients and healthy controls revealed differences in *general connectivity* in brain regions of the motor system. Compared to healthy subjects, ET patients showed a significantly increased EC in the right primary motor cortex ($P < 0.05$, FWE-corrected, Fig. 1a, red-yellow scale). We also found a cluster in the homologue region in the left hemisphere using a voxel-threshold of $P < 0.005$. Note that this cluster did not pass the FWE-correction, however, it reached significance with correction for multiple comparisons in the Lipsia software using a corrected cluster threshold of $P < 0.05$. A symmetric result is also in line with the fact that ET is a bilateral disease (see tremor assessment for the left and right arms and legs in Table 1).

When comparing EC between ET patients and healthy controls, a further significant cluster of increased EC in ET patients was found in the anterior cingulate cortex ($P < 0.05$, FWE-corrected, Fig. 1b, red-yellow scale). Using the inverse contrast of investigating reduced EC in ET patients compared with healthy controls, a significant cluster was found in the right cerebellum ($P < 0.05$, FWE-corrected, Fig. 1c, third row, blue-green scale). Here, we also found a cluster in the homologue region in the left cerebellum with using a voxel-threshold of $P < 0.005$. Note that this cluster did not pass the FWE-correction, however, it reached significance with correction for multiple comparisons in the Lipsia software using a corrected $P < 0.05$.

Our results described above were also obtained when using only positive correlations (instead of using the absolute value) when computing the EC (see Supplementary Figs. S1 and S2). Thus, EC differences can be explained by the positive correlations between fMRI time courses.

The correlation analysis between EC and FTMTS showed a significant relationship between *general connectivity* and tremor severity in ET patients. We found a significant positive correlation between FTMTS and EC in the putamen bilaterally after compensating for gender and age ($P < 0.05$, FWE-corrected, Fig. 2a, orange color). Higher connectivity was found to be associated with higher tremor severity (see Fig. 2b, correlation in the left putamen, MNI coordinate: $[-36, -1, 1]$, $r = 0.91$, $P < 10^{-7}$). Note that this positive relationship between FTMTS and EC was found in both approaches of computing EC (1) using the absolute value of the correlation between the fMRI time courses and (2) using only positive correlations setting all negative correlation values to zero (see Supplementary Fig. S3).

Selective connectivity was obtained choosing seed-regions in the

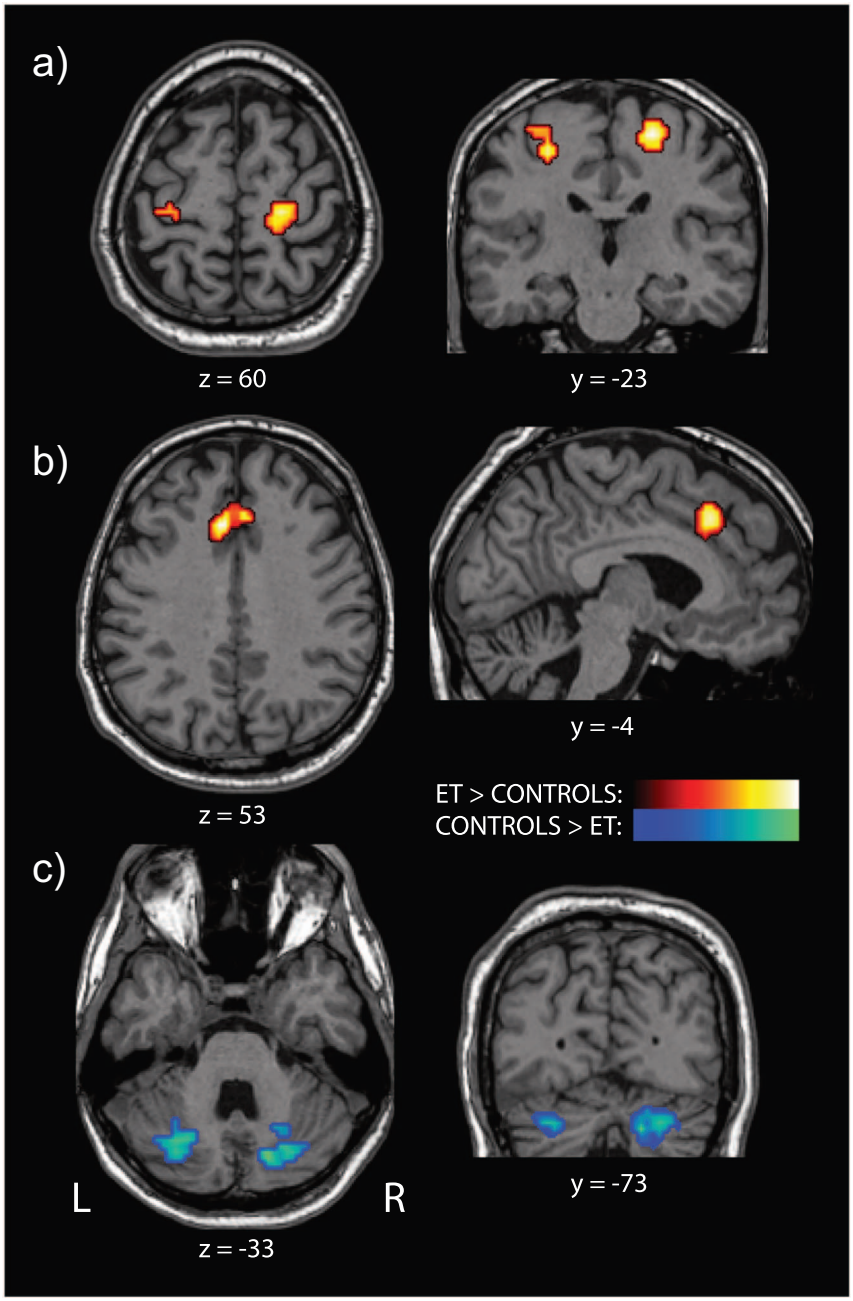

Fig. 1. Group results of resting state fMRI in patients with essential tremor (ET) (N = 19) and healthy controls (N = 23). a – primary motor cortex, b – anterior cingulate, c – cerebellum. Regions with higher eigenvector centrality (EC) in ET patients compared to healthy controls are shown in red-yellow. Regions with lower EC in ET patients than in healthy controls are shown in blue-green. Color maps were created using a voxel-wise threshold of $P < 0.005$. The clusters in the right M1, anterior cingulate and right cerebellum were significant on $P < 0.05$, FWE-corrected at cluster level. Both results in the left hemisphere (left M1, left cerebellum) were shown as significant correcting for multiple comparisons with the Lipsia software using Monte Carlo simulations with a cluster threshold of $P < 0.05$.

motor system and computing correlations between these seed-regions and all voxels within the brain. Using the coordinates of the VIM of the thalamus (Klein et al., 2012), *selective connectivity* between VIM and other brain regions was correlated with tremor severity. In particular, we found the FTMTS correlated with *selective connectivity* between VIM and basal ganglia ($P < 0.05$, FWE-corrected, Fig. 3a, blue and red color). Here we obtained an overlap in the right putamen when using the left and the right VIM as seed regions (Fig. 3a, overlap shown in white). The higher the FTMTS, i.e. the higher tremor severity, the higher the *selective connectivity* between VIM and the right putamen. Fig. 3 illustrates this correlation of the FTMTS with *selective connectivity* between the left VIM and right putamen (MNI coordinate: [24,20,1], see Fig. 3c, blue dots, $r = 0.89$, $P < 10^{-6}$), and of the FTMTS with *selective connectivity* between the right VIM and right putamen (MNI coordinate: [21, − 1,4], see Fig. 3d, red dots, $r = 0.87$, $P < 10^{-5}$).

Note that we also observed a correlation of the FTMTS with *selective connectivity* between the VIM and the left putamen using a voxel-threshold of $P < 0.005$, however, both results (using the left and right VIM as a seed region) did not reach significance after correcting for multiple comparisons (neither with the FWE approach, nor with Monte Carlo simulations using the Lipsia software).

Apart from the correlation of the FTMTS with *selective connectivity* between the VIM and the right putamen, we also found the FTMTS related to *selective connectivity* between the VIM and other brain regions including SMA and areas within the parietal lobe (Fig. 3a, blue and red color) using a voxel-threshold of $P < 0.005$. Note that these results did not pass the FWE approach, however, these clusters were obtained as significant after correction for multiple comparisons using the Lipsia software with a cluster threshold of $P < 0.05$.

In addition to use VIM as a seed region, further seed-based correlation analyses were performed. Here, seed regions were chosen in the sensorimotor system (transformed to MNI coordinates from Table 1 in (Mayka et al., 2006)). Time courses were extracted within the supplementary motor area (pre-SMA, proper-SMA), lateral premotor cortex

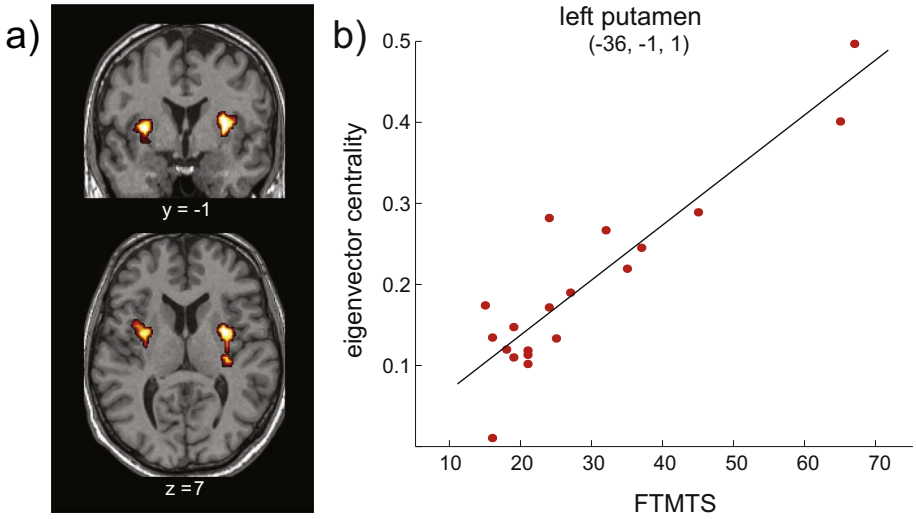

Fig. 2. Correlation of the Fahn-Tolosa-Marin Tremor Score (FTMTS) with the eigenvector centrality (EC) in patients with essential tremor (ET) ($N = 19$). a – The FTMTS positively correlated with the EC in putamen bilaterally after compensation for gender and age. Clusters were obtained using a voxel-wise threshold of $P < 0.005$ and a cluster threshold of $P < 0.05$ (FWE-corrected). b – Positive correlation between the FTMTS and EC in the left putamen ($x = -36$, $y = -1$, $z = 1$; $r = 0.91$, $P < 10^{-7}$) with compensation for gender and age.

(LPM), primary motor cortex (M1), and primary sensory cortex (S1). When using the pre-SMA as a seed region, we obtained a significant positive correlation of the FTMTS with *selective connectivity* between the pre-SMA and the basal ganglia in both hemispheres ($P < 0.05$, FWE-corrected, Fig. 4a). This positive correlation was particularly present with the *selective connectivity* between pre-SMA and putamen (Fig. 4b, MNI coordinate: [30, − 4,1], $r = 0.89$, $P < 10^{-6}$, after compensation for gender and age). Using other brain regions as a seed region (proper-SMA, LPM, M1, and S1), we did not find any significant correlation between the FTMTS and *selective connectivity* (Fig. 4c).

3.1. Motion effects

The analysis of head motion during MR scanning overall yielded

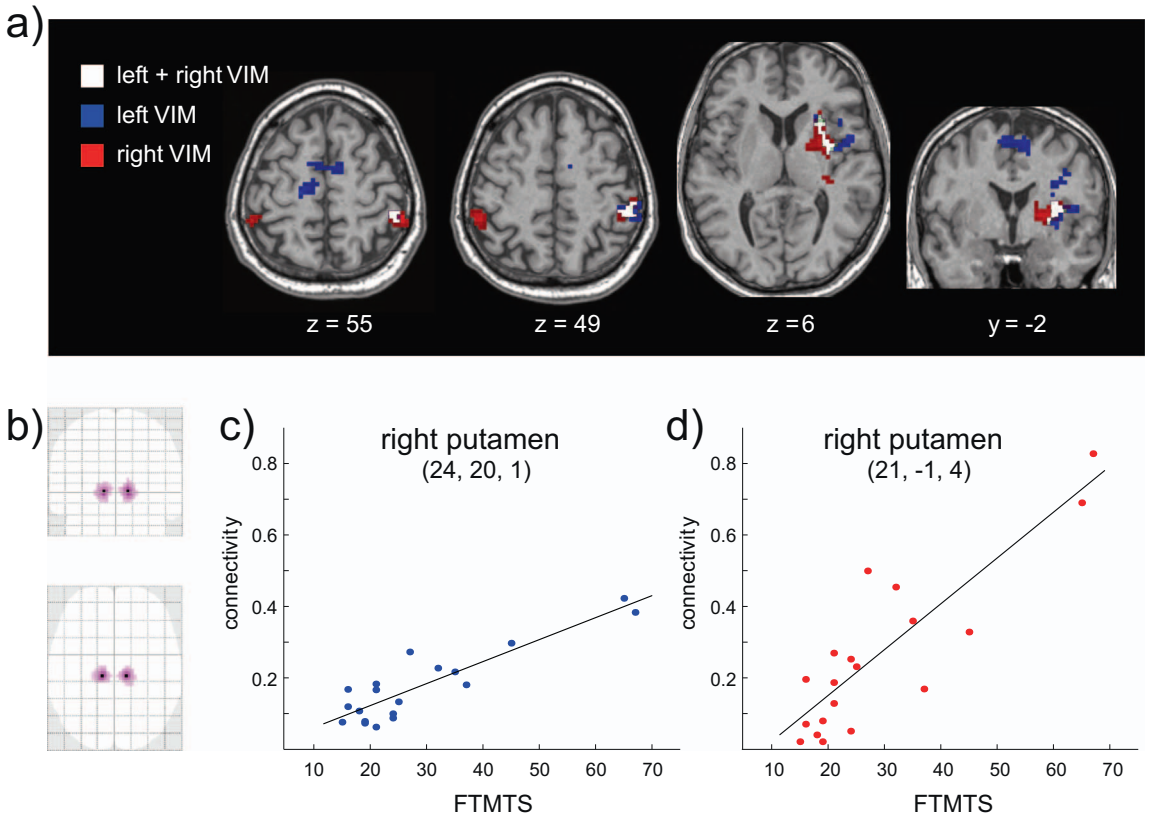

Fig. 3. Modulation of the connectivity between brain regions by the Fahn-Tolosa-Marin Tremor score (FTMTS) in patients with essential tremor (ET) ($N = 19$). Results are based on correlations of the BOLD signal between the ventral intermediate nucleus (VIM) of thalamus and the rest of the brain with gender and age used as covariates. a – The FTMTS modulated the connectivity between the left VIM (blue) or right VIM (red) and the basal ganglia. Areas with the FTMTS modulated connectivity with both VIM is in white color (voxel-wise threshold of $P < 0.005$). Both clusters in the right putamen were significant on $P < 0.05$, FWE-corrected at cluster level. The clusters in the SMA and parietal cortices were significant correcting for multiple comparisons with the Lipsia software using Monte Carlo simulations with a cluster threshold of $P < 0.05$. b – Locations of the left and right VIM of thalamus. c, d – The graph shows this modulation effect as positive correlation between the FTMTS and connectivity in the right putamen for the left VIM (blue dots, $r = 0.89$, $P < 10^{-6}$) and the right VIM (red dots, $r = 0.87$, $P < 10^{-5}$) after compensation for gender and age.

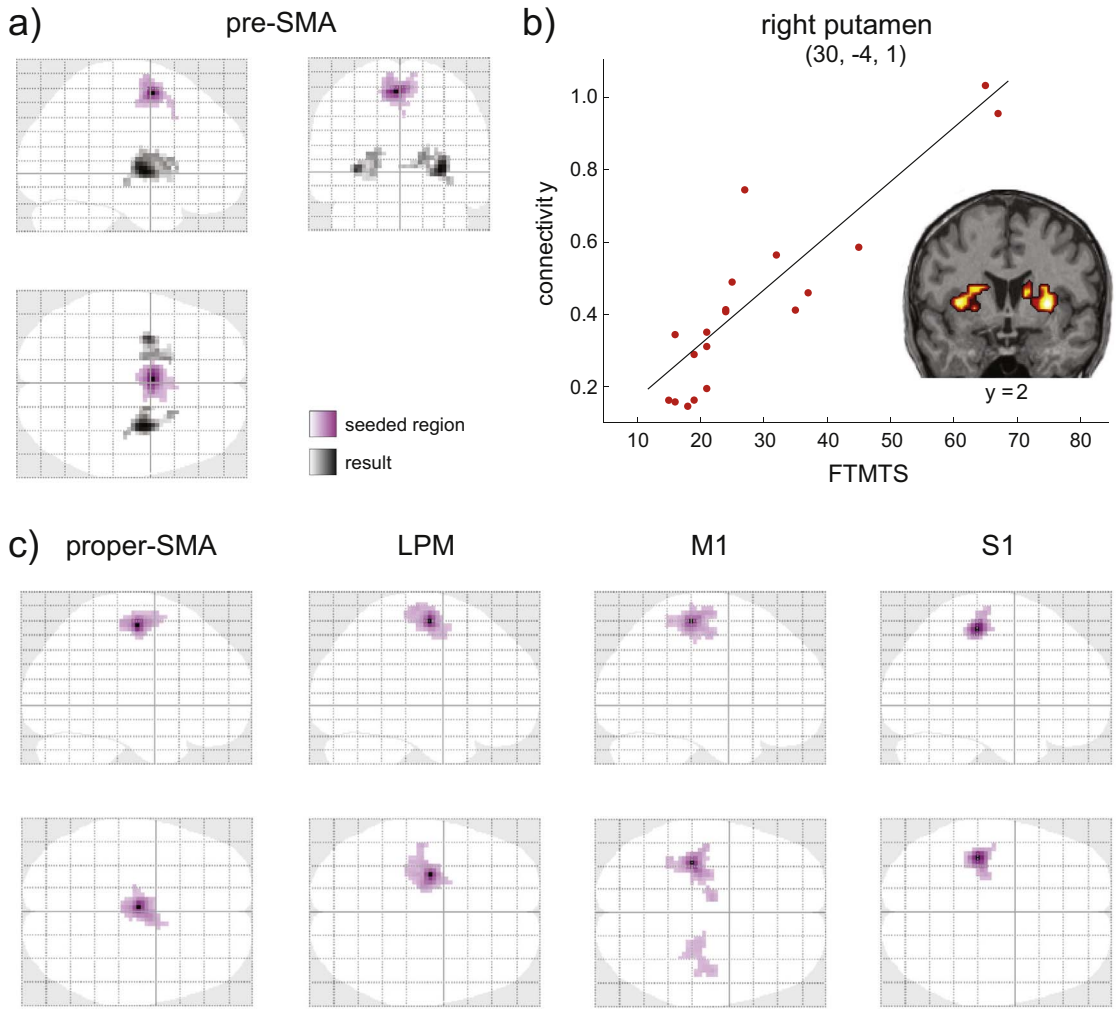

Fig. 4. Modulation of the connectivity between brain regions by the Fahn-Tolosa-Marin Tremor score (FTMTS) in patients with essential tremor (ET) ($N = 19$). Results are based on correlations of the BOLD signal between predefined seeded region and the rest of the brain. Seeded regions were chosen in the sensorimotor system (transformed to MNI coordinates from Table 1 in Mayka et al., 2006). Time courses were extracted within the supplementary motor area (pre-SMA, proper-SMA), lateral premotor cortex (LPM), primary motor cortex (M1), and primary somatosensory cortex (S1). Gender and age were used as covariates. a – The FTMTS modulated the connectivity between the pre-SMA and the basal ganglia ($P < 0.05$, FWE-corrected). b – The graph shows this modulation effect as a positive correlation between the FTMTS and connectivity ($r = 0.89$, $P < 10^{-6}$) after compensation for gender and age. The pre-SMA-basal ganglia connectivity is shown for the right putamen ($x = -30$, $y = -4$, $z = 1$). c – The FTMTS did not significantly modulate the connectivity from any other seeded regions using a voxel-wise threshold of $P < 0.005$ and a cluster threshold of $P < 0.05$ (FWE-corrected).

very subtle effects. Across all participating subjects, the mean FD was below 0.4 mm. The maximum FD was below 1.5 mm which is well below the nominal voxel dimension of our fMRI study. When disregarding the 5% largest FD values, the maximum remaining FD was < 0.7 mm. Only 6 out of 8358 frames from the entire study (i.e. 42 participants × 199 FD values) indicated single head movements by > 1 mm, corresponding to 0.07%. Moreover, we did not find any significant differences between patients and controls when investigating the mean FD ($P = 0.15$), the maximum FD ($P = 0.34$), and the maximum FD after eliminating the largest 5% of the FD values ($P = 0.82$).

Using the scrubbing technique with a relatively low FD threshold of 0.5 mm (Power et al., 2012), we obtained the same EC differences between ET patients and healthy controls (see Supplementary Figs. S4 and S5). We also obtained the same correlation between FTMTS and EC with and without scrubbing (see Fig. S6).

4. Discussion

Our results show alterations in brain connectivity of ET patients compared with healthy controls. Using EC as a measure of *general connectivity*, we found connectivity alterations between the cerebellar and other brain regions in ET which is in agreement with the concept of a functional or neurodegenerative involvement of the cerebellum in ET (Cerasa and Quattrone, 2016). Our findings are located in the same brain regions as found in other work investigating brain connectivity in ET using resting-state fMRI with other connectivity measures: Fang et al. (2013) found a diminished regional homogeneity (ReHo) in the anterior and posterior bilateral cerebellar lobes. In a later study, they used a group-wise independent component analysis (ICA) and showed a decreased functional connectivity in anterior and posterior lobes of the cerebellum (Fang et al., 2015). A similar ICA-based approach (Benito-Leon et al., 2016) showed a decreased connectivity in the cerebellar network using a dual regression technique (Filippini et al., 2009). A very recent study found a decrease of cerebellar amplitudes of low frequency fluctuations (ALFF) showing diminished low frequency fluctuations (LFOs) within the cerebellum in ET compared with healthy controls (Yin et al., 2016). Thus, our results show a common picture of cerebellar nexopathy in ET that is in line with current literature.

Apart from resting-state fMRI, ET-related cerebellar activity alterations were also found in the same brain regions identified in this study, using task-based fMRI. Using a block design with grip force task, reduced brain activity was detected in various cerebellar regions (Neely et al., 2015). In line with this finding, reduced cerebellar brain activity was also shown in ET patients using a finger tapping task (Buijink et al.,

2015). However, there are also studies showing increased cerebellar activity which appears contradictory. Nicoletti and colleagues investigated ET patients using a task with continuous writing of the number “8” with the right dominant hand and they found increased activity in the cerebellum and other brain regions of the cerebello-thalamo-cortical circuit (Nicoletti et al., 2015). Increased cerebellar activity was also found in ET patients using a working memory task (Passamonti et al., 2011). A possible interpretation of these divergent findings between a decrease and increase of brain activity might be an effect of ET related oscillations in the motor cortex in the fMRI signal. Oscillations about 3–8 Hz are related to hyperactivity in the motor cortex and while 0–3 Hz oscillations lead to hypoactivity in the cerebellum (Raethjen and Deuschl, 2012). It is also known that 0–3 Hz oscillations are related to an impairment of cerebellar-cortical functional connectivity that is in line with our observation of cerebellar EC decrease.

Our finding of a diminished EC in the cerebellum is accompanied with an increased EC in primary motor regions and the anterior cingulate cortex. The increased EC means that these regions act more like active network hubs in ET than in controls. This is in line with a current hypothesis of increased flow of information within the thalamo-cortical loop in ET leading to self-sustained oscillatory activity (Raethjen and Deuschl, 2012). Our results fit well to other studies investigating connectivity with resting-state fMRI showing an increased degree of connectivity in cortical motor and salience networks (Fang et al., 2015). Interestingly, in same brain regions, an increased ALFF was observed in ET patients (Yin et al., 2016) indicating alterations in spontaneous neural activity (Fox and Raichle, 2007). In line with these findings, ET patients also showed an increased ReHo in cortical motor regions in the left hemisphere (Fang et al., 2013). Our result of EC increase in the motor cortex also goes in line with increased brain activity in ET patients in M1 and SMA which correlated positively with 3–8 Hz oscillations (Neely et al., 2015). Findings of increased brain connectivity and activity may reflect easier propagations of slow oscillatory activity in motor circuitry of ET patients. An increased EC in cortical motor regions might be a consequence of stronger brain connectivity between putamen and cortical brain regions in parallel with dysfunctional connections projecting from/to cerebellum.

Investigating the clinical parameters in context of brain connectivity in ET, we found a positive correlation between EC and FTMTS showing an increased connectivity of the putamen of ET patients with a higher tremor severity. This means that more pronounced tremor corresponded to an increased connectivity between the putamen and other brain regions including the thalamus and SMA. This finding might be surprising because involvement of the basal ganglia is rarely reported in context with ET. As previously reported, there are mild abnormalities of striatal dopamine transporters showing a slight PD-like pattern suggesting the possible role of the basal ganglia in ET (Isaias et al., 2008). Another recent study demonstrated an involvement of the basal ganglia in context with ET therapy using beta-sympatholytics (Song et al., 2015). Patients that did not respond to propranolol therapy showed a significantly increased FTMTS together with an increased glucose metabolism in the putamen and pallidum. This finding would be in line with our result showing a positive correlation between FTMTS and EC in the putamen. Despite fundamental clinical differences, tremor generation in Parkinson's disease is associated with activity in the cerebello-thalamic circuit possibly induced by transient signals from the putamen and globus pallidus (Helmich et al., 2011). Therefore, one might speculate that an increased connectivity between the basal ganglia and cortical motor regions might be accompanied by a higher tremor severity. Interestingly, in Parkinson's disease, Helmich and colleagues describe a positive correlation between tremor severity and connectivity between the putamen and motor cortex (Helmich et al., 2011). We found a similar result showing that higher tremor severity co-varies with an increased *selective connectivity* between the putamen and pre-SMA as well as and with increased *general connectivity* of the putamen with the rest of the brain. Our results of *general connectivity* assessed by EC and *selective connectivity* assessed by voxel wise seed-based analysis might provide evidence for the possible involvement of the basal ganglia in ET. However, further work is necessary to investigate potential common pathological substrates in ET and PD.

For therapeutic intervention in ET, the ventral intermediate nucleus (VIM) of the thalamus turned out to play a central role. A first approach was suggested using thalamotomy (Hassler and Riechert, 1954; Zirh et al., 1999) with an ablation of the VIM in a surgical procedure. Later, VIM became a primary target for deep brain stimulation (DBS) to suppress tremor (Klein et al., 2012; Papavassiliou et al., 2008). Therefore, the role of the VIM needs to be investigated when analyzing alterations of brain connectivity with ET. We evaluated *selective connectivity* of the VIM using seed-based correlation analysis with rest of the brain, and we obtained a positive relationship of the FTMTS with connectivity between the left or right VIM and putamen in the right hemisphere. This correlation contributes to the increased EC in the putamen with higher tremor severity as discussed above. In another recent work, VIM was used in a seed-based correlation analysis to investigate ET-related connectivity change using resting-state fMRI (Fang et al., 2016). However, they did not obtain a relationship between tremor severity and connectivity between the VIM and basal ganglia. They report an increased connectivity between the VIM and SMA and further regions of the primary motor cortex when comparing ET patients with healthy controls (Fang et al., 2016). This is in line with our results which show a positive correlation of the FTMTS with *selective connectivity* between the VIM and SMA.

We also studied *selective connectivity* using seed regions within the motor and sensory cortices. Here we used coordinates listed in (Mayka et al., 2006) to be independent from the EC analysis (Kriegeskorte et al., 2009). We found a positive correlation of the FTMTS with connectivity between pre-SMA and putamen. A higher tremor score was found to be related to increased connectivity between these regions that is in line with our findings described above. Both putamen and SMA were found when investigating the relationship of the FTMTS with connectivity between the VIM and other brain regions. Therefore, the positive correlation of the FTMTS with connectivity between the pre-SMA and the putamen would be an expected finding. Interestingly, we did not find any FTMTS-related connectivity changes using other seed regions as the proper-SMA, the lateral premotor cortex, the primary motor cortex, and the sensorimotor cortex. However, this does not necessarily show the absence of such a relationship. Another explanation could be due to limitations of sensitivity with our approach.

To summarize, we investigated ET patients with resting-state fMRI and we found abnormal *general connectivity* expressed in alterations of eigenvector centrality showing a dysfunctional connectivity in the cerebellum but an increased connectivity with cortical motor regions. In addition, we mapped *selective connectivity* using seed-based correlation and found a relationship between tremor severity and brain connectivity related to regions that are known to be affected in ET. Our results fit very well into the current literature but also show an involvement of the basal ganglia that is a new finding aside from the current view of ET. Future studies might be aimed at further enlightenment of the complete picture of brain network alteration related to ET.

Supplementary data to this article can be found online at http://dx.doi.org/10.1016/j.nicl.2017.06.004.

Acknowledgements

The study was supported by the Czech Science Foundation (GACR16-13323S), the Czech Agency for health research (AZV16-28119A) and by Charles University in Prague (Progres Q27/LF1).

References

Ashburner, J., Friston, K.J., 2005. Unified segmentation. NeuroImage 26, 839–851.

Benito-Leon, J., Louis, E.D., Manzanedo, E., Hernandez-Tamames, J.A., Alvarez-Linera, J., Molina-Arjona, J.A., Matarazzo, M., Romero, J.P., Dominguez-Gonzalez, C., Domingo-Santos, A., Sanchez-Ferro, A., 2016. Resting state functional MRI reveals abnormal network connectivity in orthostatic tremor. Medicine (Baltimore) 95, e4310.

Binnewijzend, M.A., Adriaanse, S.M., Van der Flier, W.M., Teunissen, C.E., de Munck, J.C., Stam, C.J., Scheltens, P., van Berckel, B.N., Barkhof, F., Wink, A.M., 2014. Brain network alterations in Alzheimer's disease measured by eigenvector centrality in fMRI are related to cognition and CSF biomarkers. Hum. Brain Mapp. 35, 2383–2393.

Buijink, A.W., Broersma, M., van der Stouwe, A.M., van Wingen, G.A., Groot, P.F., Speelman, J.D., Maurits, N.M., van Rootselaar, A.F., 2015. Rhythmic finger tapping reveals cerebellar dysfunction in essential tremor. Parkinsonism Relat. Disord. 21, 383–388.

Cerasa, A., Quattrone, A., 2016. Linking essential tremor to the cerebellum-neuroimaging evidence. Cerebellum 15, 263–275.

Davey, C.E., Grayden, D.B., Egan, G.F., Johnston, L.A., 2013. Filtering induces correlation in fMRI resting state data. NeuroImage 64, 728–740.

Deuschl, G., Bain, P., Brin, M., 1998. Consensus statement of the Movement Disorder Society on Tremor. Ad Hoc Scientific Committee. Mov. Disord. 13 (Suppl. 3), 2–23.

Fahn, S., Tolosa, E., Marin, C., 1993. Clinical rating scale for tremor. In: Jankovic, J., Tolosa, E. (Eds.), Parkinson's Disease and Movement Disorders, 2nd ed. Williams & Wilkins, Baltimore, pp. 271–280.

Fang, W., Lv, F., Luo, T., Cheng, O., Liao, W., Sheng, K., Wang, X., Wu, F., Hu, Y., Luo, J., Yang, Q.X., Zhang, H., 2013. Abnormal regional homogeneity in patients with essential tremor revealed by resting-state functional MRI. PLoS One 8, e69199.

Fang, W., Chen, H., Wang, H., Zhang, H., Liu, M., Puneet, M., Lv, F., Cheng, O., Wang, X., Lu, X., Luo, T., 2015. Multiple resting-state networks are associated with tremors and cognitive features in essential tremor. Mov. Disord. 30, 1926–1936.

Fang, W., Chen, H., Wang, H., Zhang, H., Puneet, M., Liu, M., Lv, F., Luo, T., Cheng, O., Wang, X., Lu, X., 2016. Essential tremor is associated with disruption of functional connectivity in the ventral intermediate nucleus–motor cortex–cerebellum circuit. Hum. Brain Mapp. 37, 165–178.

Filippini, N., MacIntosh, B.J., Hough, M.G., Goodwin, G.M., Frisoni, G.B., Smith, S.M., Matthews, P.M., Beckmann, C.F., Mackay, C.E., 2009. Distinct patterns of brain activity in young carriers of the APOE-epsilon4 allele. Proc. Natl. Acad. Sci. U. S. A. 106, 7209–7214.

Forman, S.D., Cohen, J.D., Fitzgerald, M., Eddy, W.F., Mintun, M.A., Noll, D.C., 1995. Improved assessment of significant activation in functional magnetic resonance imaging (fMRI): use of a cluster-size threshold. Magn. Reson. Med. 33, 636–647.

Fox, M.D., Raichle, M.E., 2007. Spontaneous fluctuations in brain activity observed with functional magnetic resonance imaging. Nat. Rev. Neurosci. 8, 700–711.

Friston, K.J., Harrison, L., Penny, W., 2003. Dynamic causal modelling. NeuroImage 19, 1273–1302.

Frobenius, G., 1912. On matrices from non-negative elements. Sitzungsberichte Der Koniglich Preussischen Akademie Der Wissenschaften 456–477.

Goelman, G., Dan, R., 2017. Multiple-region directed functional connectivity based on phase delays. Hum. Brain Mapp. 38, 1374–1386.

Hassler, R., Riechert, T., 1954. Indications and localization of stereotactic brain operations. Nervenarzt 25, 441–447.

Helmich, R.C., Janssen, M.J., Oyen, W.J., Bloem, B.R., Toni, I., 2011. Pallidal dysfunction drives a cerebellothalamic circuit into Parkinson tremor. Ann. Neurol. 69, 269–281.

Holiga, S., Mueller, K., Moller, H.E., Urgosik, D., Ruzicka, E., Schroeter, M.L., Jech, R., 2015. Resting-state functional magnetic resonance imaging of the subthalamic microlesion and stimulation effects in Parkinson's disease: indications of a principal role of the brainstem. Neuroimage Clin. 9, 264–274.

Isaias, I.U., Canesi, M., Benti, R., Gerundini, P., Cilia, R., Pezzoli, G., Antonini, A., 2008. Striatal dopamine transporter abnormalities in patients with essential tremor. Nucl. Med. Commun. 29, 349–353.

Klein, J.C., Barbe, M.T., Seifried, C., Baudrexel, S., Runge, M., Maarouf, M., Gasser, T., Hattingen, E., Liebig, T., Deichmann, R., Timmermann, L., Weise, L., Hilker, R., 2012. The tremor network targeted by successful VIM deep brain stimulation in humans. Neurology 78, 787–795.

Kriegeskorte, N., Simmons, W.K., Bellgowan, P.S.F., Baker, C.I., 2009. Circular analysis in systems neuroscience — the dangers of double dipping. Nat. Neurosci. 12, 535–540.

Lohmann, G., Muller, K., Bosch, V., Mentzel, H., Hessler, S., Chen, L., Zysset, S., von Cramon, D.Y., 2001. LIPSIA—a new software system for the evaluation of functional magnetic resonance images of the human brain. Comput. Med. Imaging Graph. 25, 449–457.

Lohmann, G., Margulies, D.S., Horstmann, A., Pleger, B., Lepsien, J., Goldhahn, D., Schloegl, H., Stumvoll, M., Villringer, A., Turner, R., 2010. Eigenvector centrality mapping for analyzing connectivity patterns in fMRI data of the human brain. PLoS One 5, e10232.

Lohmann, G., Erfurth, K., Muller, K., Turner, R., 2012. Critical comments on dynamic causal modelling. NeuroImage 59, 2322–2329.

Lou, Y., Huang, P., Li, D., Cen, Z., Wang, B., Gao, J., Xuan, M., Yu, H., Zhang, M., Luo, W., 2015. Altered brain network centrality in depressed Parkinson's disease patients. Mov. Disord. 30, 1777–1784.

Mayka, M.A., Corcos, D.M., Leurgans, S.E., Vaillancourt, D.E., 2006. Three-dimensional locations and boundaries of motor and premotor cortices as defined by functional brain imaging: a meta-analysis. NeuroImage 31, 1453–1474.

Neely, K.A., Kurani, A.S., Shukla, P., Planetta, P.J., Wagle Shukla, A., Goldman, J.G., Corcos, D.M., Okun, M.S., Vaillancourt, D.E., 2015. Functional brain activity relates to 0–3 and 3–8 Hz force oscillations in essential tremor. Cereb. Cortex 25, 4191–4202.

Nichols, T., Hayasaka, S., 2003. Controlling the familywise error rate in functional neuroimaging: a comparative review. Stat. Methods Med. Res. 12, 419–446.

Nicoletti, V., Cecchi, P., Frosini, D., Pesaresi, I., Fabbri, S., Diciotti, S., Bonuccelli, U., Cosottini, M., Ceravolo, R., 2015. Morphometric and functional MRI changes in essential tremor with and without resting tremor. J. Neurol. 262, 719–728.

Obrig, H., Neufang, M., Wenzel, R., Kohl, M., Steinbrink, J., Einhaupl, K., Villringer, A., 2000. Spontaneous low frequency oscillations of cerebral hemodynamics and metabolism in human adults. NeuroImage 12, 623–639.

Papavassiliou, E., Rau, G., Heath, S., Abosch, A., Barbaro, N.M., Larson, P.S., Lamborn, K., Starr, P.A., 2008. Thalamic deep brain stimulation for essential tremor: relation of lead location to outcome. Neurosurgery 62 (Suppl. 2), 884–894.

Passamonti, L., Novellino, F., Cerasa, A., Chiriaco, C., Rocca, F., Matina, M.S., Fera, F., Quattrone, A., 2011. Altered cortical-cerebellar circuits during verbal working memory in essential tremor. Brain 134, 2274–2286.

Poline, J.B., Worsley, K.J., Evans, A.C., Friston, K.J., 1997. Combining spatial extent and peak intensity to test for activations in functional imaging. NeuroImage 5, 83–96.

Power, J.D., Barnes, K.A., Snyder, A.Z., Schlaggar, B.L., Petersen, S.E., 2012. Spurious but systematic correlations in functional connectivity MRI networks arise from subject motion. NeuroImage 59, 2142–2154.

Power, J.D., Schlaggar, B.L., Lessov-Schlaggar, C.N., Petersen, S.E., 2013. Evidence for hubs in human functional brain networks. Neuron 79, 798–813.

Qiu, T., Luo, X., Shen, Z., Huang, P., Xu, X., Zhou, J., Zhang, M., Alzheimer's Disease Neuroimaging, I., 2016. Disrupted brain network in progressive mild cognitive impairment measured by eigenvector centrality mapping is linked to cognition and cerebrospinal fluid biomarkers. J. Alzheimers Dis. 54, 1483–1493.

Raethjen, J., Deuschl, G., 2012. The oscillating central network of essential tremor. Clin. Neurophysiol. 123, 61–64.

Song, I.U., Ha, S.W., Yang, Y.S., Chung, Y.A., 2015. Differences in regional glucose metabolism of the brain measured with F-18-FDG-PET in patients with essential tremor according to their response to beta-blockers. Korean J. Radiol. 16, 967–972.

Yin, W., Lin, W., Li, W., Qian, S., Mou, X., 2016. Resting state fMRI demonstrates a disturbance of the cerebello-cortical circuit in essential tremor. Brain Topogr. 29, 412–418.

Zirh, A., Reich, S.G., Dougherty, P.M., Lenz, F.A., 1999. Stereotactic thalamotomy in the treatment of essential tremor of the upper extremity: reassessment including a blinded measure of outcome. J. Neurol. Neurosurg. Psychiatry 66, 772–775.